Vapor-Phase Direct Hydration of Ethylene over Zirconium Tungstate Catalyst

I. Catalytic Behavior and Kinetics at Atmospheric Pressure

HIROO MOMOSE, KOSHI KUSUMOTO, YUSUKE IZUMI,[1] AND YUKIO MIZUTANI

Fujisawa Research Laboratory, Tokuyama Soda Co., Ltd., 2051 Endo, Fujisawa City, Kanagawa 252, Japan

Vapor-phase direct hydration of ethylene was studied over zirconium tungstate catalyst (molar composition, W/Zr = 2.0) at atmospheric pressure. The experiments were carried out at 200–250°C, space velocity (SV) = 400–9000 h^{-1}, and H_2O/C_2H_4 mole ratio = 0.5–2.0. The optimum temperature range to give higher space-time yield (STY) of ethanol varied with the H_2O/C_2H_4 mole ratio, and the STY increased with SV up to ca. 2000 h^{-1}. The data were kinetically well interpreted by assuming that the hydration is controlled by the surface reaction between adsorbed reactants with preferential adsorption of water. Heats of adsorption were 39 kcal/mol for water and 8.5 kcal/mol for ethylene, and an apparent activation energy was 30 kcal/mol.

INTRODUCTION

During the past few decades, a number of catalysts have been proposed for direct hydration of ethylene (*1*). Among these catalysts, supported phosphoric acid has preferably been employed for industrial vapor-phase ethanol synthesis. However, the phosphoric acid catalyst still poses a problem of vaporization of acid from catalyst support during operation, which causes a decline in catalytic activity and the corrosion of equipments. Continuous feed of phosphoric acid to the catalyst zone is, therefore, needed to assure stable operation.

Tungstosilicic acid on silica gel has been offered as an alternative effective catalyst which reveals quite high activity at lower temperatures (*2*). But its activity still falls rapidly owing to acid depletion (*3*).

In order to overcome these difficulties it seems promising to use a water-insoluble catalyst, for instance, water-insoluble metal

oxides. However, most acidic metal oxide catalysts reported so far show rather low activities. $ZnO–TiO_2$ might be an exception; this binary-metal oxide catalyst described by Tanabe *et al.* (*4*) has good activity. A problem of this oxide catalyst is poor reproducibility in its preparation (*5*).

We independently attempted to design better metal oxide catalysts for ethylene hydration and found that amorphous zirconium tungstate $ZrW_{2-8}O_{0.5-3.5}$ (hereinafter referred to as ZrW), showed high catalytic activity for olefin hydration (*6*). This catalyst could be further improved by modifying the preparation method.

ZrW is an acidic binary-metal oxide and is known as an inorganic ion-exchanger in the field of analytical chemistry. According to our preliminary examination, ZrW can be prepared in various compositions of the W/Zr mole ratio, if the ratio is above unity. The ZrW having the composition of W/Zr = 2.0 showed the highest activity for ethylene hydration.

This paper is mainly concerned with the catalytic behavior of ZrW and the kinetics in the vapor-phase direct hydration of ethylene at atmospheric pressure.

[1] Present Address: Department of Synthetic Chemistry, Faculty of Engineering, Nagoya University, Furo-cho, Chikusa-ku, Nagoya 464, Japan.

EXPERIMENTAL

Reaction procedure and analysis. The reaction was carried out in a flow system using a Pyrex tubular reactor (20 × 500 mm). The catalyst (3 ml, 16–42 mesh) was placed in the middle part of the reactor and the remainder filled with porcelain Raschig rings. The tip of a C.A. thermocouple was set at the center of the catalyst bed.

The reactor was heated by an electric furnace under a nitrogen stream. When the reactor temperature exceeded 120°C, water was delivered by means of a microfeeder. The water was preheated and vaporized at the upper part of the reactor. After the reactor temperature reached a desired level and the flow of steam became steady, the nitrogen stream was switched to an ethylene stream. In the experiments for kinetic study, nitrogen was used as a diluent to adjust the partial pressures of water and ethylene. The effluent vapor from the reactor went through an ice-water trap where liquid products were collected.

The liquid and gas samples were analyzed at 1-h intervals by gas chromatography using two glass columns of PEG-1000 on Flusin T(1.5 m) and Porapak-Q(2 m). The steady formation of ethanol was usually attained after 6–24 h from the start of a run.

Ethanol was the main product through all experiments. The amounts of by-products (acetaldehyde and ethyl ether) were so small that they were measured only in cases at higher temperatures and lower space velocities.

Preparation of ZrW(W/Zr = 2.0) catalyst(7). Two aqueous solutions of Na_2WO_4(0.3 M, 2.5 liters) and $ZrOCl_2$(0.3 M, 1.25 liters) were mixed at the same time with vigorous stirring at room temperature. A white gel-like precipitate resulted. After half an hour, aqueous HCl (11.3 N, 1.25 liters) was added and stirring was continued for an additional 1 h. The slurry was then allowed to stand overnight for aging under ambient conditions. The supernatant solution was decanted and the precipitate was filtered. The wet cake was treated with an aqueous HCl(0.1 N, 5 liters) with stirring and the resultant slurry was filtered. The last procedure was repeated two or three times. The final wet cake was dried in air at 450°C for 7 h to give 216 g of glassy, pale yellow dry gel. This gel was grained and screened 16–42 mesh.

The ZrW thus prepared was characterized as amorphous and thermostable up to 560°C by X-ray and DTA analyses. The surface area and the bulk density were 100 m^2/g(by BET method) and 1.8 g/ml, respectively.

RESULTS AND DISCUSSION

Preliminary Experiments

In the earlier stage of this study, various water-insoluble metal oxides were prepared and tested for ethylene hydration activity at atmospheric pressure. These metal oxides include zirconium phosphates (P/Zr mole ratio = 1.0, 2.0, and 4.0), zirconium salts of heteropoly acids such as tungstophosphoric acid and tungstosilicic acid, zirconium molybdates (Mo/Zr = 1.0 and 2.0), tungsten oxide supported on zirconia, and other binary-metal oxides such as WO_3–ZnO and WO_3–SnO_2, as well as ZrW that was prepared by our earlier method or its modification devised in the present study (vide supra).

Among these catalysts tested, only ZrW revealed similar or higher catalytic activity compared with widely used supported phosphoric acid catalyst. A ZrW of W/Zr = 2.0 (ZrW-II-(B)) prepared by the modified method was the most effective, in particular (Table 1). The modified method is different from the earlier one chiefly in the conditions of washing and drying of the wet cake of ZrW. The method is superior in reproducibility, too.

Catalytic Behavior of Zirconium Tungstate

In order to clarify the catalytic behavior of ZrW, the effects of reaction temperature,

TABLE 1

Catalytic Activities of Various Zirconium Tungstates and Supported Phosphoric Acid for the Vapor Phase Direct Hydration of Ethylene at Atmospheric Pressure

Catalyst	Temperature (°C)	EtOH concentration[a] (wt%)
Zirconium tungstate[b]		
ZrW-I-(A)	220	0.38
ZrW-I-(B)	220	0.60
ZrW-II-(A)	220	0.74
	245	0.70
ZrW-II-(B)	220	0.90
	245	0.81
ZrW-III-(B)	220	0.80
Supported H_3PO_4[c]	220	0.45
	245	0.59

[a] Concentration of ethanol in the liquid sample under the conditions of H_2O/C_2H_4 (mole ratio) = 1.0 and SV = 2300 h^{-1}.

[b] I, W/Zr (mole ratio) = 1.0; II, W/Zr = 2.0; III, W/Zr = 3.0; (A), previous preparation method (6); (B), present modified method.

[c] Nikki Chem. Co., N-501.

H_2O/C_2H_4 mole ratio, and space velocity on the hydration activity were studied using the ZrW-II-(B) catalyst.

Figure 1 shows the change of space-time yield(STY) of ethanol with temperature at different H_2O/C_2H_4 ratios under a constant space velocity. At each H_2O/C_2H_4 ratio, the STY increased with temperature, passed through a maximum, and then decreased owing to equilibrium limitation. The temperature to give a maximum STY, however, varied depending on H_2O/C_2H_4 ratio; the lower the ratio, the lower the optimum temperature. Below 215°C, lower H_2O/C_2H_4 ratios gave higher STY. The STY computed from equilibrium ethylene conversion should be largest at H_2O/C_2H_4 ratio = 1.0 and identical at 0.5 and 2.0, if the conversion is very small (dashed lines denoted in Fig. 1). In accord with this theoretical prediction, the observed STY was highest at the ratio = 1.0 in the range of temperature above 240°C where ethylene conversions were ruled by equilibrium.

However, no observed STY ever reached the theoretical ones, and the yields at H_2O/C_2H_4 ratio = 0.5 and 2.0 still differed from each other. These results suggest the retardation of the reaction by strong and selective adsorption of one of the reactants onto the catalyst surface, which will be discussed again in the kinetic study.

Acetaldehyde, probably formed by the dehydrogenation of ethanol, became detectable apparently after the reaction temperature exceeded those giving the maximum ethanol STY. However, the amount was quite small (0.5–3.0% of ethanol by weight) in any case.

Figure 2 shows the effect of space velocity on STYs of ethanol and acetaldehyde at 220°C and H_2O/C_2H_4 = 1.0. The ethanol STY increased with space velocity in a manner similar to the theoretical STY curve (a dashed line) up to about 2000 h^{-1}, and then gradually leveled off. On the other hand, the STY of acetaldehyde rapidly decreased with increasing space velocity and became negligibly small above 3000 h^{-1}.

Kinetics

In order to interpret the catalytic behavior of ZrW in detail, the kinetic experiments were performed using ZrW-II-(B) catalyst.

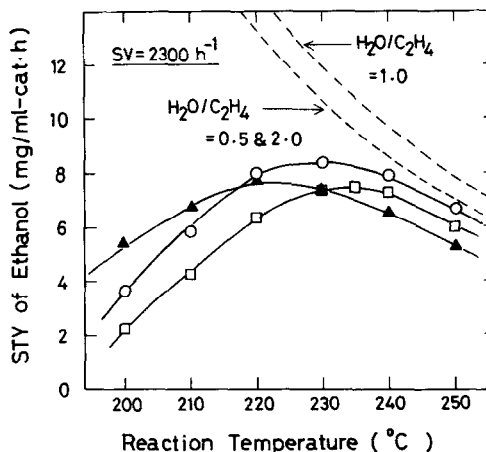FIG. 1. Temperature dependence of space-time yield of ethanol. Space velocity, 2300 h^{-1}; H_2O/C_2H_4 mole ratio, 0.5 (▲), 1.0 (○), 2.0 (□); (---), STY at equilibrium conversion.
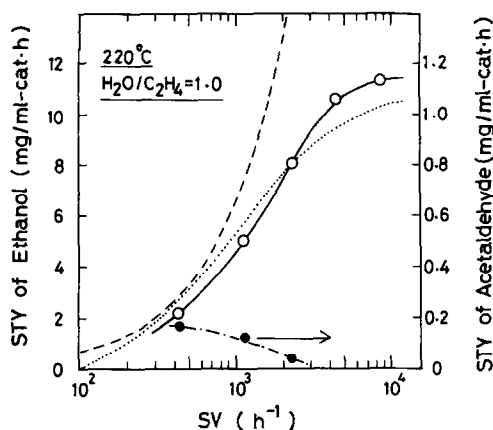
FIG. 2. Space-time yields of ethanol and acetaldehyde vs space velocity. Temperature, 220°C; H_2O/C_2H_4 mole ratio, 1.0; (O), ethanol; (●), acetaldehyde; (– – –), ethanol STY at equilibrium conversion; (······), ethanol STY calculated from Eq. (9).

There have been rather few reports concerning detailed kinetics of ethylene hydration. Mace and Bonilla (8) investigated the vapor-phase reaction at elevated pressures over WO_3/SiO_2 and WO_3/Al_2O_3 catalysts, and established a rate equation for the hydration reaction. They assumed the Langmuir–Hinshelwood mechanism and indicated that the hydration proceeded via the surface reaction with no preferential adsorption by ethylene or water and with no strong retardation by ethanol adsorption. Ono and Sugiura (9) analyzed the reaction over a supported phosphoric acid catalyst. Although they conducted the reaction in the vapor phase, they showed that a rate equation based on a homogeneous system could be applicable because phosphoric acid might exist in the form of a condensed liquid (10) on the catalyst support.

ZrW is an insoluble solid catalyst like WO_3/SiO_2, and a usual gas–solid heterogeneous reaction should proceed on the catalyst surface. In the present study, therefore, the kinetic data were analyzed following Mace and Bonilla (8). Since little diffusional resistance was observed under the present reaction conditions, only chemical reaction processes were kinetically taken into account.

When reaction (1) is represented by A + B = R and

$$H_2O(g) + C_2H_4(g) = C_2H_5OH(g) \quad (1)$$
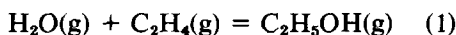
the surface reaction is assumed rate controlling, and the net reaction rate is:

$$r = ZK_AK_B(f_Af_B - f_R/K_f)/$$
$$(1 + f_AK_A + f_BK_B + f_RK_R)^2 \quad (2)$$

where r = net reaction rate (mol – R/ml-cat · h), Z = overall rate constant for surface reaction, K_A, K_B, K_R = adsorption equilibrium constants of the respective components (atm^{-1}), f_A, f_B, f_R = fugacities of the respective components at the interface (atm), which are assumed equal to the fugacities in the main gas stream, K_f = equilibrium constant of the hydration reaction in terms of fugacity (atm^{-1}).

Equation (2) is integrated by relating r to fugacity f_R by the material balance $rdV = FdN_R \doteq FN_{R(f)}/f_{R(f)} df_R$ and holding f_A and f_B constant at their average values, $f_{A(a)}$ and $f_{B(a)}$, since they do not change much during a run. V, F, N_R, $N_{R(f)}$, and $f_{R(f)}$ denote volume of catalyst (ml), total feed rate at inlet (mol/h), moles of ethanol formed per moles of total feed, final N_R at outlet, and final f_R at outlet, respectively. Also, f_RK_R in the denominator in Eq. (2) is neglected because f_R is small compared with f_A and f_B, and K_R would be expected to be small compared with K_A and K_B, as shown later. Thus the integration gives:

$$(-U)^{-1/2} = (FK_fN_{R(f)}/VZf_{R(f)}K_AK_B)^{1/2}$$
$$(1 + f_{A(a)}K_A + f_{B(a)}K_B) \quad (3)$$

where

$$U = -\ln(1 - f_{R(f)}/f_{A(a)}f_{B(a)}K_f).$$

Similarly, the rate equation for the ethylene adsorption controlling and its integrated form are given:

$$r = Z_B(f_B - f_R/f_AK_f)/$$
$$(1 + f_AK_A + f_RK_R + f_RK_B/f_AK_f) \quad (4)$$

and

$$(-U)^{-1} = K_f(f_{A(a)} + f_{A(a)}f_{B(a)} + f_{A(a)}^2 K_A)/$$
$$(f_{R(f)}K_B + VZ_B f_{R(f)}/FN_{R(f)}) \quad (5)$$

respectively, where Z_B is the overall rate constant. Exchange of suffixes A and B in Eqs. (4) and (5) leads to the corresponding equations for the water adsorption controlling. For the ethanol desorption controlling, Eq. (6) and its integrated form Eq. (7) are obtained:

$$r = Z_R(f_A f_B K_f - f_R)/$$
$$(1 + f_A K_A + f_B K_B + f_A f_B K_R K_f) \quad (6)$$

$$(-U)^{-1} = FN_{R(f)}(1 + f_{A(a)}K_A + f_{B(a)}K_B$$
$$+ f_{A(a)}f_{B(a)}K_R K_f)/VZ_R f_{R(f)}. \quad (7)$$

Now, when initial fugacity of water or ethylene at inlet is varied while the other is fixed at a given temperature and a space velocity, the following relationships will be expected because each initial fugacity is almost equal to the corresponding average value, $f_{A(a)}$ or $f_{B(a)}$, at small conversions, and $f_{R(f)}/N_{R(f)}$ is approximated to the total pressure (=1 atm):

(i) $(-U)^{-1/2}$ should be linear in terms of each fugacity, $f_{A(a)}$ or $f_{B(a)}$, if the surface reaction is rate-controlling (Eq. (3)),

(ii) $(-U)^{-1}$ should be linear in terms of each fugacity if the ethanol desorption is rate-controlling (Eq. (7)), and

TABLE 2

Kinetic Data at a Constant Space Velocity of 2300 h^{-1}

Temperature (°C)	$f_{A(a)}$ (atm)	$f_{B(a)}$ (atm)	Concn[a] (wt%)	STY[b] $\left(\dfrac{\text{mg-EtOH}}{\text{ml-cat} \cdot \text{h}}\right)$	$f_{R(f)}^{c} \times 10^4$ (atm)	$(-U)^{-1}$	$(-U)^{-1/2}$
190	0.30	0.15	0.170	0.94	1.99	5.58	2.36
190	0.30	0.30	0.330	1.82	3.87	5.76	2.40
190	0.30	0.45	0.460	2.54	5.40	6.24	2.50
190	0.30	0.60	0.580	3.20	6.80	6.63	2.58
190	0.64	0.30	0.092	1.07	2.29	22.0	4.69
190	0.47	0.30	0.160	1.37	2.91	12.4	3.53
200	0.30	0.15	0.270	1.50	3.18	2.41	1.55
200	0.30	0.30	0.490	2.73	5.77	2.72	1.65
200	0.30	0.50	0.740	4.12	8.71	3.06	1.75
200	0.30	0.70	0.930	5.18	10.9	3.47	1.86
200	0.68	0.30	0.160	2.01	4.24	9.47	3.08
200	0.46	0.30	0.290	2.47	5.21	4.99	2.23
210	0.30	0.15	0.360	2.01	4.22	1.17	1.08
210	0.30	0.45	0.890	4.97	10.4	1.55	1.25
210	0.30	0.60	1.08	6.03	12.7	1.77	1.33
210	0.62	0.30	0.340	3.90	8.20	3.15	1.78
210	0.47	0.30	0.450	3.94	8.28	2.24	1.50
210	0.31	0.30	0.650	3.74	7.86	1.36	1.17
220	0.30	0.15	0.390	2.15	4.57	0.64	0.80
220	0.30	0.30	0.720	3.97	8.44	0.76	0.87
220	0.30	0.45	0.990	5.46	11.6	0.90	0.95
220	0.30	0.60	1.22	6.73	14.3	1.03	1.02
220	0.58	0.30	0.540	5.71	12.1	1.25	1.12
220	0.45	0.30	0.620	5.14	10.9	1.00	1.00

[a] Concentration of ethanol in the liquid sample.
[b] STY $\doteq$ (mg-feed water/h) $\times$ (concentration of ethanol[a])/100/(ml-catalyst).
[c] $f_{R(f)} \doteq$ (moles of ethanol produced) $\times$ 1 atm/(moles of total feed).

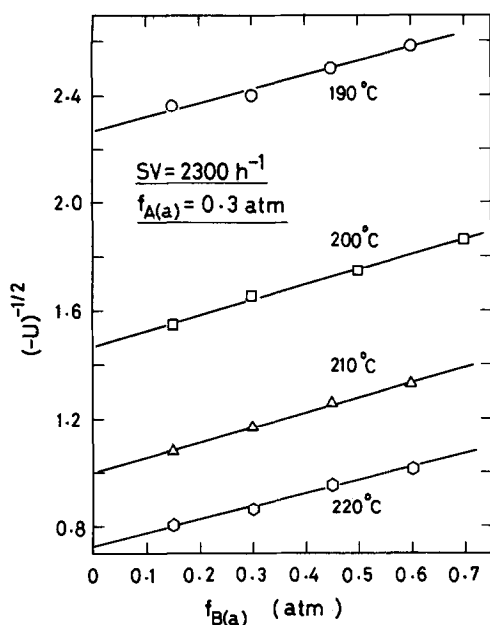FIG. 3. Plots of $(-U)^{-1/2}$ vs ethylene fugacity at water fugacity of 0.3 atm.

(iii)   no simple linear relationships should be found in case of adsorption controlling, but, for example, $(-U)^{-1}$ becomes either linear with $f_{B(a)}$ or second-ordered with $f_{A(a)}$, if $f_{R(f)}K_B$ in Eq. (5) is neglected.

Thus a probable rate-controlling step may be known by examining the relationships among $(-U)^{-1/2}$, $(-U)^{-1}$, $f_{A(a)}$, and $f_{B(a)}$.

According to Ewell's equation to estimate the fugacity coefficient (11), $\ln \gamma = (9/128) [(PT_c/P_cT)(1 - 6T_c^2/T^2)]$, each of the fugacity coefficients of water, ethylene, and ethanol is almost unity (>0.99) at 1 atm and above 190°C. Hence the partial pressures can be substituted for the corresponding fugacities in Eqs. (3), (5), and (7).

In every run, one of the partial pressures of the reactants was held constant at 0.3 atm while the other was varied from 0.3 to ca. 0.7 atm at 190–220°C, and space velocity was fixed at 2300 h^{-1} throughout all experiments. The values of $f_{R(f)}$ were evaluated from the concentrations of ethanol in the liquid products. Equilibrium constants,

K_f, were estimated from thermodynamic data by Ewell's method (11).

The kinetic results are summarized in Table 2. The rate expression of either the surface reaction control or the ethylene adsorption control fairly well interprets the kinetic data as indicated by the linear relationships illustrated in Figs. 3, 4, and 5 as well as implied by the second-order dependence of $(-U)^{-1}$ on $f_{A(a)}$ in Fig. 6. On the other hand, the ethanol desorption is unlikely to control the reaction because $(-U)^{-1}$ did not change linearly with $f_{A(a)}$ as shown in Fig. 6.

In order to judge which is more probable between the surface reaction control and the ethylene adsorption control, the values of Z, Z_B, K_A, and K_B were computed and listed in Table 3, using the kinetic data in Table 2 by means of least-squares. It is reasonably inferred that the ethylene adsorption control mechanism should be ruled out, because the K_A value became negative at 220°C and moreover both K_B and Z_B had maximum values between 190 and 220°C. On the other hand, the result based on Eq.
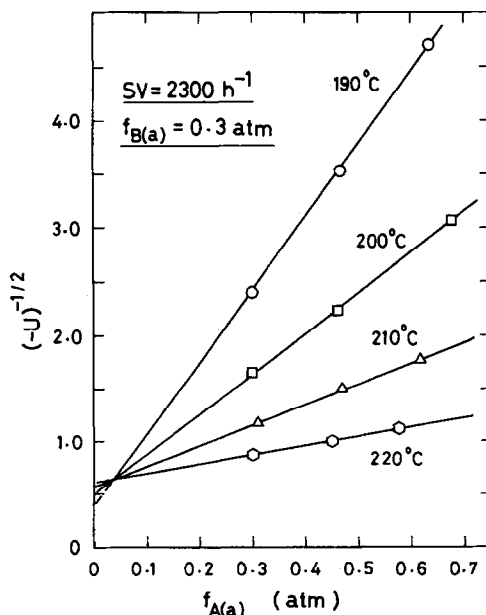

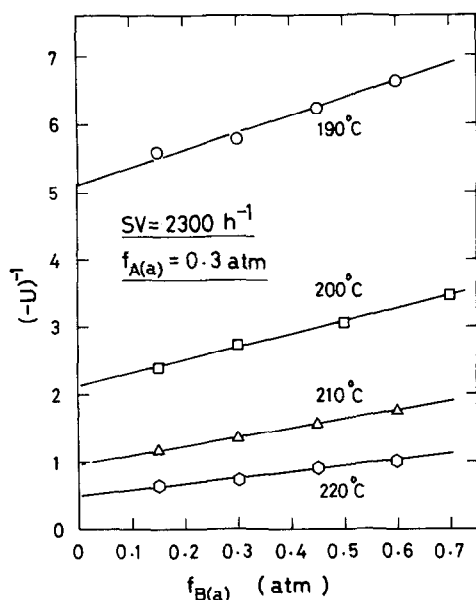FIG. 4. Plots of $(-U)^{-1/2}$ vs water fugacity at ethylene fugacity of 0.3 atm.

FIG. 5. Plots of $(-U)^{-1}$ vs ethylene fugacity at water fugacity of 0.3 atm.
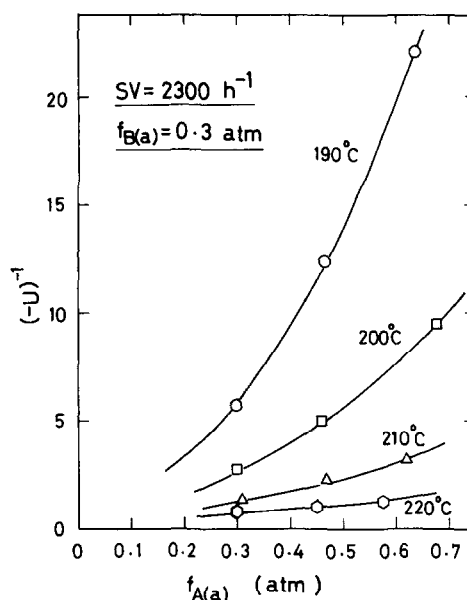
FIG. 6. Plots of $(-U)^{-1}$ vs water fugacity at ethylene fugacity of 0.3 atm.

(3) is numerically rational, which may lead to a conclusion that the reaction rate is probably determined by the surface reaction. The heats of adsorption for water and ethylene were estimated from the temperature dependence of K_A and K_B shown in Fig. 7. They were 39 and 8.5 kcal/mol, respectively. Large K_A values at lower temperatures well meet our expectation that ZrW should have stronger affinity for water than for ethylene owing to the nature of ion-exchangers. In addition, a significant nu-

merical difference observed between K_A and K_B except for their values at around 235°C supports an earlier suggestion about preferential adsorption of water or ethylene onto the catalyst. At temperatures below ca. 235°C (estimated from Fig. 7), water is adsorbed more preferably than ethylene. Since an Arrhenius plot for the rate constant Z was a curve in shape as shown in Fig. 7, an activation energy of the reaction could not be estimated at this stage. The reason may be explained in terms of a con-

TABLE 3

Adsorption Equilibrium Constants and Overall Rate Constants

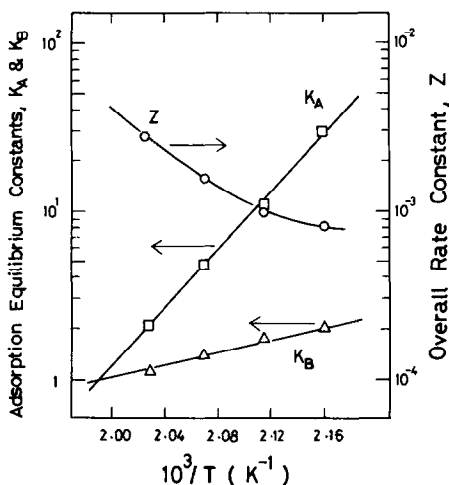| Temperature (°C)	Surface reaction controlling (from Eq. (3))			Ethylene adsorption controlling (from Eq. (5))		
	K_A (atm^{-1})	K_B (atm^{-1})	$Z \times 10^3$ $\left(\dfrac{\text{mol-EtOH}}{\text{ml-cat} \cdot \text{h}}\right)$	K_A (atm^{-1})	K_B (atm^{-1})	$Z_B \times 10^3$ $\left(\dfrac{\text{mol-EtOH}}{\text{ml-cat} \cdot \text{h}}\right)$
190	27.8	2.03	0.82	12.3	24.1	0.73
200	11.4	1.68	1.01	9.14	27.7	1.19
210	4.81	1.39	1.53	1.83	10.2	0.88
220	2.10	1.16	2.80	−0.43	5.67	0.81

FIG. 7. Arrhenius plots of adsorption equilibrium constants (water, K_A and ethylene, K_B) and overall rate constant (Z).

tinuous decrease in the number of active sites with temperature; i.e., some side reactions such as polymerization of ethylene and/or acetaldehyde might foul the catalyst surface. Indeed, acetaldehyde was detected in all kinetic runs, and its amount, though limited, increased with temperature.

Kinetic Review on Overall Catalytic Behavior

Since the above kinetic study has been done within rather limited reaction conditions, it seems necessary to examine whether all the results obtained in the wider ranges of space velocity and temperature may also be kinetically well interpreted on the basis of Eq. (3).

For small conversions under ideal piston flow conditions, the ethanol STY(mg-EtOH/ml-cat · h) can be expressed by:

$$STY = (FN_{R(0)}M_w/V) \times 1000 \qquad (8)$$

where M_w is the molecular weight of ethanol. Because $f_{R(0)}/N_{R(0)}$ is nearly 1 atm, we can substitute $f_{R(0)}$ for $N_{R(0)}$ in Eq. (8) to give:

$$STY = [\{FK_f M_w f_{A(a)} f_{B(a)}/V \cdot 1(\text{atm})\}$$
$$\{1 - 1/\exp(VZK_A K_B/FK_f(1 + K_A f_{A(a)} + K_B f_{B(a)})^2)\}] \times 1000 \qquad (9)$$

using $f_{R(0)}$ derived from Eq. (3) which represents an integral rate expression for the surface reaction control.

First, the results shown in Fig. 1 were reexamined, where the reaction temperature ranged from 200 to 250°C. The numerical values of K_A and K_B above 220°C were estimated by extrapolation of the kinetic data in Fig. 7. Using the observed STY in Fig. 1, the overall rate constant Z can be calculated from Eq. (9) for each H_2O/C_2H_4 mole ratio in the range between 200 and 250°C. The results are summarized in Table 4. Apparently, the calculated Z values are in good agreement with each other at each temperature irrespective of H_2O/C_2H_4 mole ratios. The average Z values ($\bigcirc$) below 220°C were also in good agreement with the corresponding Z values observed in the independently performed kinetic experiments ($\bullet$). An apparent activation energy of the reaction was approximately 30 kcal/mol above 220°C; the value was obtained from an Arrhenius plot in Fig. 8. Mace and Bonilla also reported 30 kcal/mol for an activation energy of the reaction over WO_3/SiO_2 catalyst (8).

Second, the results shown in Fig. 2 were reexamined, where space velocity was varied. The ethanol STY calculated from Eq.
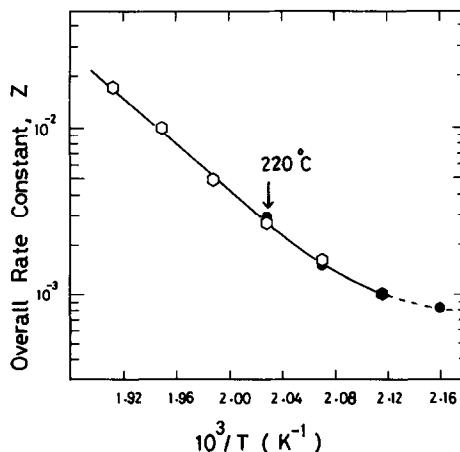

FIG. 8. Arrhenius plot of overall rate constant (Z). ($\bigcirc$), average values calculated from Eq. (9) and observed STY in Fig. 1; ($\bullet$), values obtained in the kinetic experiments.

TABLE 4

Z Values Calculated from Eq. (9)

Temperature (°C)	$K_f{}^a \times 10^2$ (atm^{-1})	K_A (atm^{-1})	K_B (atm^{-1})	$Z \times 10^3$ (mol-EtOH/ml-cat · h)			
				$m^c = 0.5$	$m = 1.0$	$m = 2.0$	av
190	2.70	27.8	2.03	—	—	—	—
200	2.08	11.4	1.68	1.1	1.0	1.0	1.0
210	1.63	4.81	1.39	1.6	1.6	1.6	1.6
220	1.28	2.10	1.16	2.8	2.8	2.6	2.7
230	1.02	0.96^b	0.98^b	4.9	5.0	4.9	4.9
240	0.82	0.45^b	0.83^b	9.2	10	10	9.7
250	0.66	0.22^b	0.71^b	16	18	17	17

^{a} Values calculated by Ewell's method (11).
^{b} Values estimated from Fig. 7.
^{c} m = H_2O/C_2H_4 mole ratio.

(9) is illustrated in Fig. 2 as a dotted line and compared with the observed STY (a solid line). Considering that the calculated STY is based on the estimated values of K_A, K_B, and Z, and moreover that the effect of space velocity on acetaldehyde formation is disregarded, the kinetic expression for STY of Eq. (9) may be said to be able to rather well represent the observed STY.

It is, therefore, concluded that all the results obtained in the present study on the ethylene hydration over ZrW were kinetically well interpreted by assuming that the reaction is controlled by the surface reaction between adsorbed water and ethylene.

REFERENCES

1. (a) Berkman, S., Morrell, J. C., and Egloff, G., "Catalysis." Reinhold, New York, 1940; (b) Ogino, Y., Sekiyu Gakkai Shi 17, 166 (1974).

2. (a) Muller, J., and Waterman, H. I., Brennstoff-Chem. 38, 321 (1957); (b) Kurita, M., Hosoya, T., Uchida, H., Imai, T., and Yoshinaga, Y., J. Nat. Chem. Lab. Ind. 61, 218 (1966).

3. Kuribayashi, H., and Kugo, M., Kogyo Kagaku Zasshi 69, 1930 (1966).

4. Tanabe, K., Ishiya, C., Matsuzaki, I., Ichikawa, I., and Hattori, H., Bull. Chem. Soc. Japan 45, 47 (1972).

5. Tanabe, K., J. Synthetic Org. Chem. Japan 33, 842 (1975).

6. (a) Mizutani, Y., and Ihara, H., Brit. Pat. 1,192,692; (b) Mizutani, Y., and Ihara, H., USP 3,450,777.

7. Kusumoto, K., Momose, H., Izumi, Y., and Mizutani, Y., Japan Kokai Tokkyo Koho 79 57,500.

8. Mace, C. V., and Bonilla, C. F., Chem. Eng. Progr. 50, 385 (1954).

9. Ono, R., and Sugiura, T., Sekiyu Gakkai Shi 14, 984 (1971).

10. Handlos, A. E., and Nixon, A. C., Ind. Eng. Chem. 48, 1960 (1956).

11. Ewell, R. H., Ind. Eng. Chem. 32, 147 (1940).